Dynamic Visualization of Nanoscale Vortex Orbits

Matias Timmermans,[†,§] Tomas Samuely,[†,‡,§] Bart Raes,[†,⊥] Joris Van de Vondel,[†] and Victor V. Moshchalkov[†,*]

[†]INPAC—Institute for Nanoscale Physics and Chemistry, KU Leuven, Celestijnenlaan 200D, B-3001 Leuven, Belgium and [‡]Centre of Low Temperature Physics, Institute of Physics, P. J. Šafárik University, Park Angelinum 9, 04001 Košice, Slovakia. [§]M. Timmermans and T. Samuely contributed equally. [⊥]Present address: Physics and Engineering of Nano Electronic Devices Group, Catalan Institute of Nanotechnology, Campus Universidad Autónoma de Barcelona, E-08193 Bellaterra, Spain.

ABSTRACT Due to the atomic-scale resolution, scanning tunneling microscopy is an ideal technique to observe the smallest objects. Nevertheless, it suffers from very long capturing times in order to investigate dynamic processes at the nanoscale. We address this issue, for vortex matter in $NbSe_2$, by driving the vortices using an ac magnetic field and probing the induced periodic tunnel current modulations. Our results reveal different dynamical modes of the driven vortex lattices. In addition, by recording and synchronizing the time evolution of the tunneling current at each pixel, we visualize the overall dynamics of the vortex lattice with submillisecond time resolution and subnanometer spatial resolution.

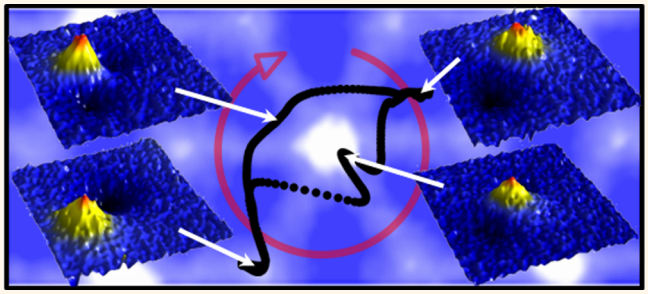

KEYWORDS: scanning tunneling microscopy · superconductivity · dynamics · vortex

The dynamics of nanoscale objects forms a very interesting field of research with a strong technological impact.[1,2] The ability to control these processes (*e.g.*, by electromagnetic field,[3,4] current,[5] temperature,[6] photoisomerization,[7] or chemically[8]) brings us closer to constructing useful nanodevices. To fully understand and exploit such systems, their direct visualization is vital. Still, a technique resolving (sub)nanometer particles within a time frame relevant to observe dynamics is a very challenging task.[9−13] We demonstrate the direct visualization of a controlled motion of nanoobjects: superconducting vortices in $NbSe_2$ driven by ac magnetic field. In order to do so, we introduce a novel approach to the scanning tunneling microscopy (STM). Invented by Binning and Rohrer in the early 1980s, STM has proven to be a very powerful technique to probe various physical systems on an atomic length scale,[14] including the superconducting state. This started with the visualization of the Abrikosov vortex lattice in $NbSe_2$.[15] This experiment directly demonstrated the power of STM as a tool to investigate a static superconducting condensate with unprecedented atomic resolution: to name a few, studies of the nature of high-temperature superconductivity,[16] the electronic properties of the vortex cores,[17,18] and the observation of periodic local density of states modulations in the superconducting state.[19] While these "static" studies are invaluable in order to understand the origin of superconductivity, a similar investigation of the time evolution of the condensate is of utmost importance to reveal the mechanisms responsible for energy dissipation.[20,21] Therefore, the experimental observation of the superconducting condensate, on a relevant time scale, opens a new route to determine the mechanisms involved and enables new insights into the dynamics of vortex matter.[22−24] In order to study dynamic events, contrary to its outstanding spatial resolution, STM is usually limited by its poor time resolution (*ca.* 10 s per image). As a result, one can investigate only dynamic events that are slow[25,26] with respect to the stroboscopic sampling time determined by the time necessary to acquire an image. Our new STM approach makes it possible to map the dynamics of vortices with unprecedented time (<1 ms) and spatial resolution (<1 nm).

RESULTS AND DISCUSSION

It is apparent from Figure 1a and b that our STM is capable of obtaining the energy and spatial resolution needed to visualize

* Address correspondence to victor.moshchalkov@fys.kuleuven.be.

Received for review December 19, 2013 and accepted January 27, 2014.

Published online January 27, 2014
10.1021/nn4065007

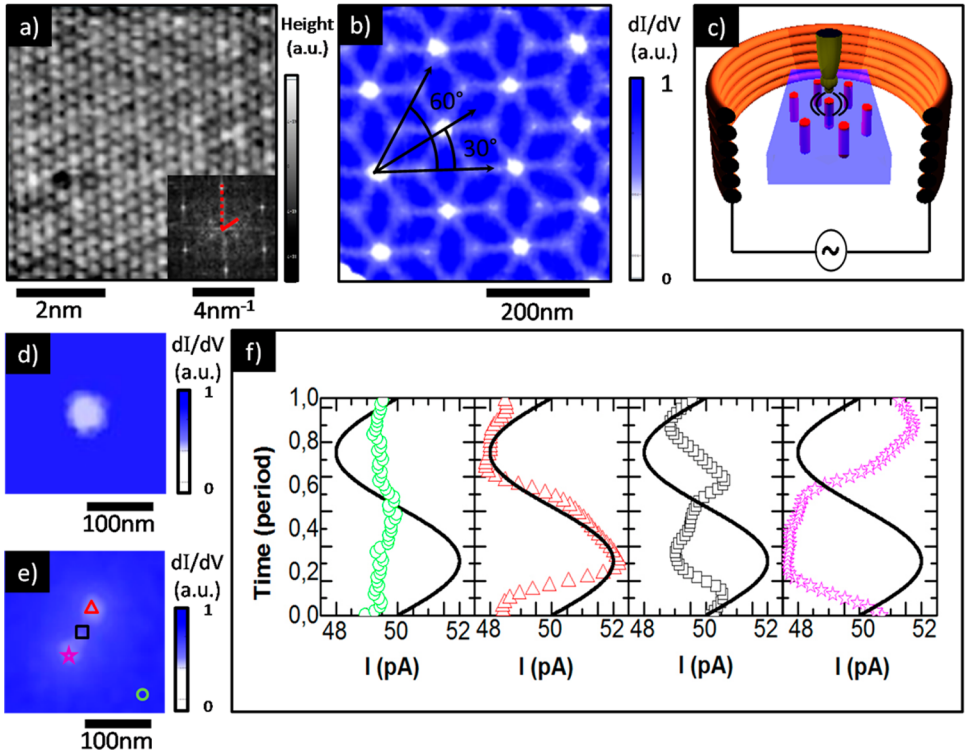

Figure 1. (a) Hexagonal atomic lattice of Se atoms at the surface of a cleaved $NbSe_2$ single crystal together with the presence of a charge density wave that creates a superimposed modulation every three Se atoms, as reported previously in many other STM experiments.[32] The corresponding Fourier transform (inset) reveals the characteristic wave vectors of the atomic (dashed red line) and charge density wave (CDW) modulations (full red line) in reciprocal space. The image is taken in constant current mode with $\langle I_T \rangle = 50$ pA and $V_{bias} = 0.89$ mV at $T = 1.3$ K, with an *in situ* prepared Au tip. (b) Conductance map at $V_{bias} = 0.89$ mV taken in constant current mode $\langle I_T \rangle = 120$ pA, using a bias modulation of $V_{mod} = 60$ μV_{rms} with frequency $f = 3.123$ kHz, showing the vortex lattice obtained by performing a field-cooled measurement in $B_{dc} = 100$ mT at $T = 0.71$ K. The observed star-shaped depletion of the condensate due to the kinetic energy of the superconducting condensate, surrounding each vortex, is clearly visible at this bias voltage.[17] The black arrows are aligned with the atomic lattice with a principle axis at 30°. (c) Schematic presentation of the measurement setup. (d) Conductance map of a single vortex. (e) Conductance map of the vortex in (d) subjected to an ac magnetic field with amplitude $B_{ac} = 0.127$ mT and frequency $f = 77.357$ Hz, resulting in an elongated vortex shape. (f) Tunneling current *versus* time at four different locations as marked by the green, red, black, and blue symbols in (e). The induced ac driving force is added as a reference signal (solid line).

vortices and atoms simultaneously. To move vortices, the most common method is the application of an external current through the sample. This is difficult to realize in an STM, because the applied current will make reliable and accurate measurements problematic.[27,28] To avoid this problem, a periodic driving force is created indirectly by applying an alternating magnetic field (Figure 1c). The induced screening currents drive the vortices periodically. In order to confirm the presence of this motion, we have a closer look at the conductance map with and without an applied ac field (Figure 1d and e). The specifically chosen slow scanning speed (39 ms/pixel) ensures that every pixel of the conductance map is the average value of the conductance at the given location over three periods of the ac drive, in analogy with long-exposure photography. The smearing of the vortex core clearly demonstrates that the vortex is moving.

The aforementioned scans of the superconducting state were obtained in the well-known constant current mode, using a tip−sample distance feedback loop. However, if the condensate changes with a speed exceeding the settling time of the feedback loop, tunnel current modulations will be present around the average value. This is experimentally verified at four different locations of the sample (Figure 1f). These measurements show that the induced vortex motion results in a variation of the tunneling current, I_T, while away from the vortex the tunneling current remains constant. Moreover, the periodicity of the modulations shows the potential of using a lock-in technique to track the motion of vortices with superior precision. (See Supporting Information for method description.)

Figure 2 shows two representative (out of 15) measurements of the conductance (Figure 2a and b) and the in-phase component (Figure 2c and d) of the first-harmonic lock-in signal when an ac drive is applied. Although the vortex lattice is shifted between consecutive measurements, the orientation of the vortex lattice remains unchanged, and it is aligned with the atomic lattice (Figure 2e).[22,23] This demonstrates that the atomic lattice contributes substantially to the potential landscape. Due to the small ac drive ($B_{ac} = 0.4\%$ of B_{dc}), the smearing of the gap is undetectable in the

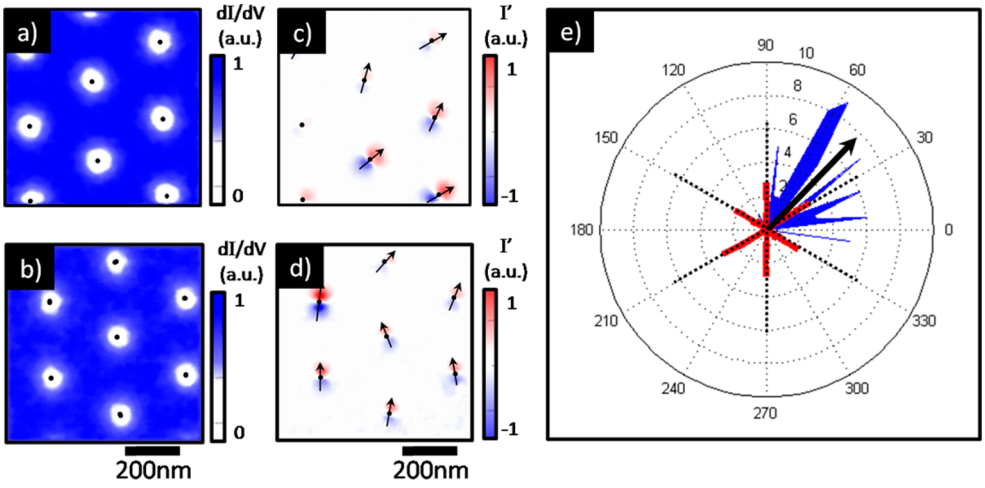

Figure 2. Conductance maps (a, b) and the measured in-phase component (c, d) of the first harmonic, I', of consecutive prepared vortex lattices while an ac drive of 0.127 mT is applied with a frequency of $f = 77.357$ Hz. Both states are prepared by a field-cooling procedure to $T = 2$ K in a dc magnetic field of 30 mT. A red zone in (c) and (d) indicates that a vortex is moving in-phase with the applied ac drive within this area, while a blue spot indicates antiphase motion in accordance with Figure 1f. (e) Polar plot of all obtained principal Abrikosov lattice vectors (red) and the shaking directions of the full data set (blue). The dashed lines reflect the atomic lattice vectors obtained from Figure 1a. The arrow indicates the average oscillation direction, which is a good estimate of the driving force direction.

conductance map; however a clear fingerprint of oscillatory motion is observed in the first harmonic of the tunnel current signal. The lock-in technique, although not reaching its full potential, is able to detect vortex motion with amplitudes lower than 5 nm. For these weak ac drives, a linear approximation[29] has been widely used in the literature, and the in-phase component of the tunnel current is expected to present a good picture of the vortex motion. The observed vortex oscillations are clearly inhomogeneous, in both amplitude and direction (Figure 2e), with a strong enhancement around 60°. These observations directly prove the presence of both disorder and anisotropy in the potential landscape.

As the next step, we investigated the influence of the density of particles on their dynamics by increasing the dc field (Figure 3a–d). A transition takes place from individual to collective oscillations of the vortices around B_{dc} = 80 mT. This collective and coherent motion of the vortex lattice, shown in Figure 3a, is evidenced by a unidirectional oscillatory motion of all vortices within a single scan area. The crossover to this collective regime can be explained by the increasing importance of the vortex–vortex interaction upon decreasing the intervortex distance. In addition to this, measurements show that in most cases the average oscillatory direction is along one of the principal axes of the vortex lattice (*i.e.*, 30°), whereas the estimated drive direction is 46° (Figure 2e). This is in accordance with the notion that the vortices in the collective regime are guided along channels that are stable against the transversal force component.[25,26] This channeled motion has been explained by the presence of a "tin roof potential" induced by the interplay between the atomic lattice of $NbSe_2$ and the vortex lattice,[25] both having 6-fold symmetry. Intriguingly, the preferred direction of oscillation, 60°, observed in the single vortex regime (Figure 2e) differs from the 30° observed in the collective regime (Figure 3).

Upon increasing the dc field value, first, the displacement of the vortices is enhanced, resulting in the smearing of the vortex signal in the conductance map (Figure 3b top panel). When the lattice oscillation reaches one lattice constant, the smearing disappears in the conductance map while the in-phase signal becomes very weak (Figure 3c bottom panel). This is a direct observation of so-called "mode-locking" between the distance traveled by a single vortex and the underlying periodicity of the vortex lattice.[30] As anticipated, this effect results in a strong enhancement of the second harmonic signal (Figure 3 insets bottom panels). Finally, the vortex displacement exceeds the lattice constant, and again a clear signal is present in the first harmonic (Figure 3d). In this case the time evolution at a certain location is determined by the passage of more than one vortex and the physical meaning of the first harmonic becomes complicated. Nevertheless, the presence of a stripe pattern in the conductance map, aligned with the principal axes of the vortex lattice, confirms the presence of a "tin roof potential" for the moving vortex lattice in the collective regime.

The characteristic features of the first and the second Fourier component clearly show that in a wide range of magnetic fields and amplitudes each vortex follows a well-defined periodic trace during each ac cycle. This periodic motion can be probed using an extended version of the so-called "Lazy fisherman method",[31] in which a fisher (tip) waits at a fixed position for a fish (vortex) to pass by. In our case, we will put the fisher at

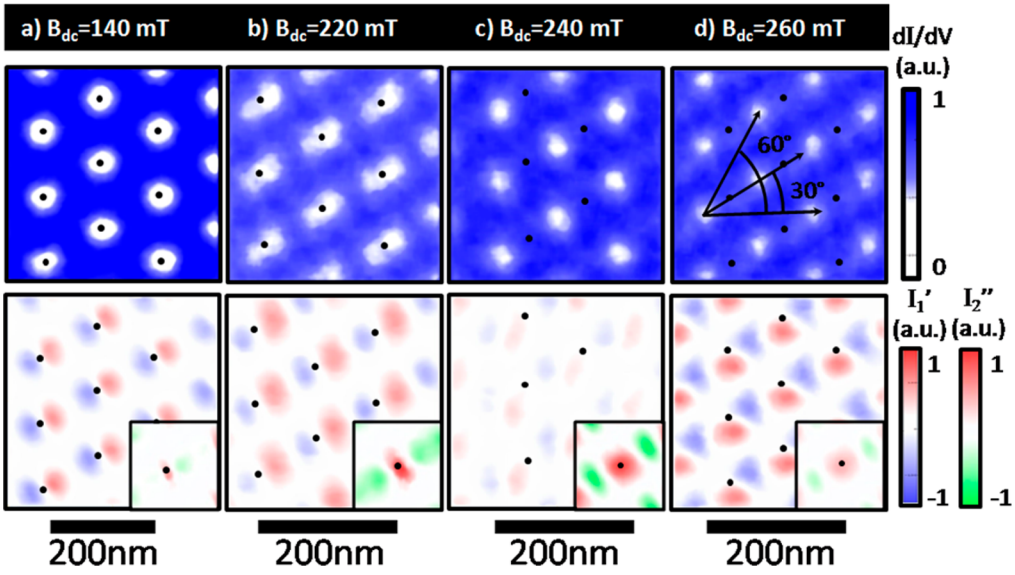

Figure 3. Vortex density dependence of the ac dynamics at certain representative magnetic field values, obtained by exciting a vortex distribution, prepared by a field-cooling process, to a temperature of 2 K in dc magnetic fields ranging from 30 to 500 mT. The conductance map (top) and the first (botom) and second (inset) harmonic are measured while the prepared state is subjected to an excitation with an ac magnetic field of B_{ac} = 0.127 mT at a frequency of f = 77.357 Hz. The black dots mark the center of mass for each oscillating vortex.

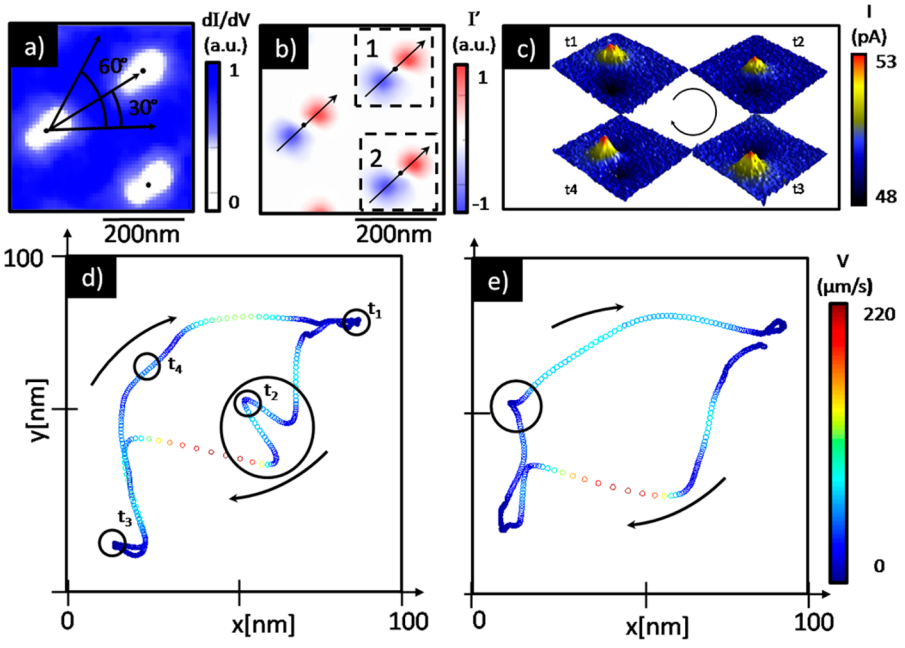

Figure 4. (a) Conductance map of a prepared vortex lattice while an ac drive of 0.152 mT is applied with a frequency of f = 77.357 Hz. The state is prepared by a field-cooling procedure to T = 3.2 K in a dc magnetic field of 30 mT. (b) Measured in-phase component of the I_T first harmonic. (c) Two-dimensional map of the tunnel current as a function of four different times marked in (d). (d and e) Two-dimensional vortex orbits at two different locations labeled in (b), respectively. The color code shows the vortex velocity at each point.

work to fish at each pixel during a few cycles of the vortex motion, while using the ac reference signal to set the time frame. By combining all curves obtained for each pixel (I_T *versus* time) we can construct a two-dimensional map of the tunnel current as a function of time (Figure 4c and supplementary videos). These maps can be used to determine the trace and the velocity of the vortex motion.

An example of the visualization of such a motion is given in Figure 4d and e. It reveals that the actual trajectory of a vortex is in fact a nanoscale orbit with radius ~50 nm. These findings indicate that the average trace (Figure 4a) and the first harmonic (Figure 4b) give only an approximate idea about the vortex trajectory. By comparing two different vortices we can see that the nanoscale orbit is a common phenomenon

and, as such, can be attributed to the potential induced by the atomic and/or vortex lattice. In addition, as shown in Figure 4d (encircled region), differences in the vortex orbit appear because defects can trap a vortex along its orbit. The shape of the orbit indicates that the vortex avoids moving along the principal axis (30°). At higher vortex densities (Figure 3) this was exactly the direction of the average vortex motion. This additional anisotropy within the "tin roof potential", only revealed by our superior time resolution, implies that the vortex motion is much more subtle than previously thought. We propose a tentative explanation for the intricate shape of the vortex trajectory. By carefully analyzing Figure 1b, it is evident that along the principal axes the condensate is enhanced, while channels of depletion are present at 0° and 60°. Each vortex is repelled by the areas of enhanced superconductivity, which results in an additional anisotropy along 0° and 60° on top of the "tin roof potential". In this manner, both the nanoscale orbit and the observed anisotropy in the single vortex regime (Figure 2e) can be explained as a consequence of the "tin roof potential" combined with the additional anisotropy stemming from the existence of the superconducting depletion channels.

CONCLUSION AND OUTLOOK

In the presented work, we investigated the controlled periodic motion of superconducting vortices in $NbSe_2$. In order to inspect this dynamic process, we introduced a novel approach to the traditional STM measurements, not dissimilar to the "lazy fisherman" technique,[31] but more elaborate. Within this novel approach, two distinct techniques can be distinguished. By means of the first technique, using a lock-in amplifier, we were able to determine the direction and amplitude of oscillating vortices, with respect to the Abrikosov lattice. Confronting the behavior of the vortices oscillating individually with small amplitudes, with the behavior of the vortices oscillating collectively with larger amplitudes, resulted in a puzzling discrepancy. Namely, the preferred orientation in the collective regime was along the principal axis of the Abrikosov lattice, in accordance with the previously observed "tin roof" potential,[26] in contrast to the single vortex regime, where the vortices tended to avoid this direction. However, by employing the second technique, we were able to address this issue in more detail. This second technique enabled us to dynamically visualize the trajectory of the moving vortices by constructing real-time videos. This was done by combining and synchronizing the time evolution of the tunneling current recorded at each point of the scanned area. From these videos, it is evident that, in the collective regime, the vortex trajectory is a nano-orbit, with the onset along the channels of depleted superconductivity, avoiding the main axis of the Abrikosov lattice, in accordance with the single-vortex regime. This clarification was possible due to the eminent spatial resolution of the introduced techniques and also due to the ability to dynamically visualize the processes involved. From a more general point of view, this approach can be extended to any scanning probe microscopy technique investigating dynamic processes that are periodic, either spontaneously[6] or where the periodicity is imposable by external control.[3−5]

MATERIALS AND METHODS

All the experiments were performed on a freshly cleaved 2H-$NbSe_2$ crystal by means of the Attocube scanning tunneling microscope cryomagnetic system, with a ^{3}He refrigerator reaching a base temperature of 300 mK. A standard resistive counter-heater with a feedback loop was employed to maintain a stable temperature above the base. A superconducting coil was used to provide a dc magnetic field up to 7 T. An extra copper coil fitted around the STM head inside the vacuum shield provided the ac magnetic field. An EG & G Instruments 7265 DSP lock-in amplifier was used to directly obtain d*I*/d*V* values. A Stanford Research Systems SR830 DSP lock-in amplifier was employed in the lock-in technique. The techniques introduced in this work are described in more detail in the Supporting Information, section 1.

Conflict of Interest: The authors declare no competing financial interest.

Acknowledgment. We acknowledge support from the Methusalem funding by the Flemish government, FWO, and the MP1201 COST-action projects. T.S. would like to acknowledge the Slovak R&D agency contract no. APVV-0036-11.

Supporting Information Available: Supplementary videos of the moving vortices: 30mT_3p2K_12 mA.AVI and 30mT_3K_9 mA.AVI. Supporting information about the techniques used. This material is available free of charge *via* the Internet at http://pubs.acs.org.

REFERENCES AND NOTES

1. Labayen, M.; Ramirez, C.; Schattke, W.; Magnussen, O. M. Quasi-Collective Motion of Nanoscale Metal Strings in Metal Surfaces. *Nat. Mater.* **2003**, *2*, 783–787.
2. Schaffert, J.; Cottin, M. C.; Sonntag, A.; Karacuban, H.; Bobisch, C. A.; Lorente, N.; Gauyacq, J.-P.; Möller, R. Imaging the Dynamics of Individually Adsorbed Molecules. *Nat. Mater.* **2013**, *12*, 223–227.
3. Neumann, J.; Gottschalk, K. E.; Astumian, D. R. Driving and Controlling Molecular Surface Rotors with a Terahertz Electric Field. *ACS Nano* **2012**, *6*, 5242–5248.
4. Seldenthuis, J. S.; Prins, F.; Thijssen, J. M.; van der Zant, H. S. J. An All-Electric Single-Molecule Motor. *ACS Nano* **2010**, *4*, 6681–6686.
5. Jorn, R.; Zhao, J.; Petek, H.; Seideman, T. Current-Driven Dynamics in Molecular Junctions: Endohedral Fullerenes. *ACS Nano* **2011**, *5*, 7858–7865.
6. Pelling, E.; Sehati, S.; Gralla, E. B.; Valentine, J. S.; Gimzewski, J. K. Local Nanomechanical Motion of the Cell Wall of Saccharomyces cerevisiae. *Science* **2004**, *305*, 1147–1150.
7. Cho, J.; Berbil-Bautista, L.; Pechenezhskiy, I. V.; Levy, N.; Meier, S. K.; Srinivasan, V.; Kanai, Y.; Grossman, J. C.; Vollhardt, K. P. C.; Crommie, M. F. Single-Molecule-Resolved Structural Changes Induced by Temperature and Light in Surface-Bound Organometallic Molecules Designed for Energy Storage. *ACS Nano* **2011**, *5*, 3701–3706.
8. Nguyen, T. D.; Glotzer, S. C. Reconfigurable Assemblies of Shape-Changing Nanorods. *ACS Nano* **2010**, *4*, 2585–2594.

9. van Houselt, A.; Zandvliet, H. J. W. Colloguium: Time-Resolved Scanning Tunneling Microscopy. *Rev. Mod. Phys.* **2010**, *82*, 1593–1605.
10. Swartzentruber, B. S. Direct Measurement of Surface Diffusion Using Atom-Tracking Scanning Tunneling Microscopy. *Phys. Rev. Lett.* **1996**, *76*, 459–462.
11. Kramer, R. B. G.; Ataklti, G. W.; Moshchalkov, V. V.; Silhanek, A. V. Direct Visualization of the Campbell Regime in Superconducting Stripes. *Phys. Rev. B* **2010**, *81*, 144508.
12. Raes, B.; Van de Vondel, J.; Silhanek, A. V.; de Souza Silva, C. C.; Gutierrez, J.; Kramer, R. B. G.; Moshchalkov, V. V. Local Mapping of Dissipative Vortex Motion. *Phys. Rev. B* **2012**, *86*, 064522.
13. Vasyukov, D.; Anahory, Y.; Embon, L.; Halbertal, D.; Cuppens, J.; Ne'eman, L.; Finkler, A.; Segev, Y.; Myasoedov, Y.; Rappaport, M. L.; *et al.* Scanning Nano-SQUID with Single Electron Spin Sensitivity. *Nat. Nanotechnol.* **2013**, *8*, 639–644.
14. Binnig, G.; Rohrer, H. In Touch with Atoms. *Rev. Mod. Phys.* **1999**, *71*, 324–330.
15. Hess, H. F.; Robinson, R. B.; Dynes, R. C.; Valles, J. M., Jr.; Waszczak, J. V. Scanning-Tunneling-Microscope Observation of the Abrikosov Flux Lattice and the Density of States near and inside a Fluxoid. *Phys. Rev. Lett.* **1989**, *62*, 214–216.
16. Fischer, Ø.; Kugler, M.; Maggio-Aprile, I.; Berthod, C.; Renner, C. Scanning Tunneling Spectroscopy of High-Temperature Superconductors. *Rev. Mod. Phys.* **2007**, *79*, 353–419.
17. Hess, H. F.; Robinson, R. B.; Waszczak, J. V. Vortex-Core Structure Observed with a Scanning Tunneling Microscope. *Phys. Rev. Lett.* **1990**, *64*, 2711–2714.
18. Guillamón, I.; Suderow, H.; Vieira, S.; Cario, L.; Diener, P.; Rodière, P. Superconducting Density of States and Vortex Cores of 2H-NbS_2. *Phys. Rev. Lett.* **2008**, *101*, 166407.
19. Guillamon, I.; Suderow, H.; Guinea, F.; Vieira, S. Intrinsic Atomic-Scale Modulations of the Superconducting Gap of 2H-$NbSe_2$. *Phys. Rev. B* **2008**, *77*, 134505.
20. Bardeen, J.; Stephen, M. J. Theory of Motion of Vortices in Superconductors. *Phys. Rev.* **1965**, *140*, 1197–1207.
21. Tinkham, M. Viscous Flow of Flux in Type-II Superconductors. *Phys. Rev. Lett.* **1964**, *13*, 804–807.
22. Villegas, J. E.; Savel'ev, S.; Nori, F.; Gonzalez, E. M.; Anguita, J. V.; García, R.; Vicent, J. L. A Superconducting Reversible Rectifier That Controls the Motion of Magnetic Flux Quanta. *Science* **2003**, *302*, 1188–1191.
23. de Souza Silva, C. C.; Van de Vondel, J.; Morelle, M.; Moshchalkov, V. V. Controlled Multiple Reversals of a Ratchet Effect. *Nature* **2006**, *440*, 651–654.
24. Van de Vondel, J.; Gladilin, V. N.; Silhanek, A. V.; Gillijns, W.; Tempere, J.; Devreese, J. T.; Moshchalkov, V. V. Vortex Core Deformation and Stepper-Motor Ratchet Behavior in a Superconducting Aluminum Film Containing an Array of Holes. *Phys. Rev. Lett.* **2011**, *106*, 137003.
25. Troyanovski, A. M.; Aarts, J.; Kes, P. H. Collective and Plastic Vortex Motion in Superconductors at High Flux Densities. *Nature* **1999**, *399*, 665–668.
26. Lee, J.; Wang, H.; Dreyer, M.; Berger, H.; Barker, B. I. Nonuniform and Coherent Motion of Superconducting Vortices in the Picometer-Per-Second Regime. *Phys. Rev. B* **2011**, *84*, 060515.
27. Maldonado, A.; Guillamón, I.; Suderow, H.; Vieira, S. Scanning Tunneling Spectroscopy under Large Current Flow through the Sample. *Rev. Sci. Instrum.* **2011**, *82*, 073710.
28. Maldonado, A.; Vieira, S.; Suderow, H. Supercurrent on a Vortex Core in 2H-$NbSe_2$: Current Driven Scanning Tunneling Spectroscopy. *Phys. Rev. B* **2013**, *88*, 064518.
29. Campbell, A. M. The Interaction Distance between Flux Lines and Pinning Centres. *J. Phys. C* **1971**, *4*, 3186–3198.
30. Olson, C. J.; Reichhardt, C.; Nori, F. Nonequilibrium Dynamic Phase Diagram for Vortex Lattices. *Phys. Rev. Lett.* **1998**, *81*, 3757–3760.
31. Kohen, A.; Cren, T.; Proslier, Th.; Noat, Y.; Sacks, W.; Roditchev, D.; Giubileo, F.; Bobba, F.; Cucolo, A. M.; Zhigadlo, S. M.; *et al.* Superconducting Vortex Profile From Fixed Point Measurements the "Lazy Fisherman" Tunneling Microscopy Method. *Appl. Phys. Lett.* **2005**, *86*, 212503.
32. Sacks, W.; Roditchev, D.; Klein, J. Voltage-Dependent STM Image of a Charge Density Wave. *Phys. Rev. B* **1998**, *57*, 13118–13131.